Journal of Structural Geology 31 (2009) 44–54

Contents lists available at ScienceDirect

Journal of Structural Geology

journal homepage: www.elsevier.com/locate/jsg

Structural controls on a carbon dioxide-driven mud volcano field in the Northern Apennines (Pieve Santo Stefano, Italy): Relations with pre-existing steep discontinuities and seismicity

Marco Bonini*

Consiglio Nazionale delle Ricerche (CNR), Istituto di Geoscienze e Georisorse (IGG), Via G. La Pira 4, I-50121 Florence, Italy

ARTICLE INFO

Article history:
Received 9 January 2008
Received in revised form 29 July 2008
Accepted 1 October 2008
Available online 1 November 2008

Keywords:
Carbon dioxide
Mud volcanism
Fluid circulation and fluid pressure
Faults
Pre-existing brittle fabrics
Seismicity
Northern Apennines

ABSTRACT

The strong release of carbon dioxide (CO_2)-rich fluids in the axial zone of the Northern Apennines, near Pieve Santo Stefano, is analysed in relation to both structural controls and the microseismicity that followed the earthquake of 26 November 2001. Some vents recorded a transition from gas-dominated emission to post-seismic mud extrusion. The co-seismic rupture of a portion of the NW-trending Alto Tiberina Fault, which bounds the Quaternary Upper Tiber Basin, presumably broke the hydraulic seal trapping overpressured CO_2-rich fluid compartments and released a fluid pressure pulse. Fault pattern analysis has revealed that venting localises along NE-trending steep faults associated with the regional transverse Arbia-Val Marecchia Line bounding the basin to the northwest. It is proposed that the transverse faults have been acting as permeable pathways allowing the post-seismic transport of over-pressured fluids to the surface, during which the mud was mobilised. A hypothetical correlation is also established between failure mechanisms and the 2001 aftershocks. Results of Mohr constructions indicate that frictional fault reactivation is a suitable mechanism for explaining the seismic events along the NW-trending normal fault, while hydraulic fracturing is the most suitable to describe the seismicity occurring along the transverse faults.

1. Introduction and aims of the work

Mud volcanoes are temporary structures emitting saline water (often containing a liquid hydrocarbon part), mud, and gases. Though methane rising from hydrocarbon traps is frequently the dominating gas fraction, mud volcanoes can be also driven by carbon dioxide (e.g., Milkov, 2000; Kopf, 2002; Mazzini et al., 2007) liberated from metamorphic reactions affecting carbonates, or resulting from magmatic rocks and mantle degassing (e.g., Minissale, 2004). Gases expelled from mud volcanoes may thus have a great relevance for gas flux input to the geosphere and the consequent impact on the greenhouse effect (e.g., Etiope et al., 2004; Minissale, 2004).

Carbon dioxide (CO_2) emissions are normally indicative of a deep origin, and thus manifest the occurrence of permeable pathways connecting the surface down to upper crustal levels. This paper examines the structural conditions of a CO_2-driven mud volcano field settled in the axial zone of Northern Apennines, between Caprese Michelangelo and Pieve Santo Stefano, along the upper course of Tiber River (Fig. 1). This field represents an excellent case history for studying the relations between the emission of deep origin fluids and structural controls for several reasons: (1) the existence of the deep well "Pieve Santo Stefano 1" (PSS-1) within the venting area establishes the physical conditions of trapped fluids; (2) the venting area is located close to the seismically-active faults bounding the Upper Tiber Basin; (3) the occurrence of a seismic crisis (with epicentre located less than 10 km from the vents) has strongly influenced the venting style; and (4) the availability of geochemical analyses of expelled fluids. Moreover, the presence of high-pressure CO_2-rich fluids trapped at depth may generate aftershock sequences, as documented in the near Umbria–Marche Apennines (Miller et al., 2004).

The Pieve Santo Stefano mud volcano field has experienced a recent increase in gas and fluid flow that has been attributed to increased fluid pressure associated with the earthquake that shocked the area on the 26 November 2001 (Heinicke et al., 2006). Such an earthquake has been related to the rupture of a segment of the NW-trending normal fault (known as the Alto Tiberina Fault) bounding the nearby Upper Tiber Basin (Heinicke et al., 2006; Fig. 1b). However, the definition of structures controlling surface venting is complex, as fluid seeps essentially coincide with ~NE-trending steep transverse fault segments pre-dating the development of the Upper Tiber Basin and bounding this basin to the northwest (Fig. 1b,c). Accordingly, the observation that surface seepage is controlled by brittle faults allows tackling the more

* Corresponding author. Tel.: +39 055 275 7528; fax: +39 055 290 312.
E-mail address: mbonini@geo.unifi.it

0191-8141/$ – see front matter © 2008 Elsevier Ltd. All rights reserved.
doi:10.1016/j.jsg.2008.10.003

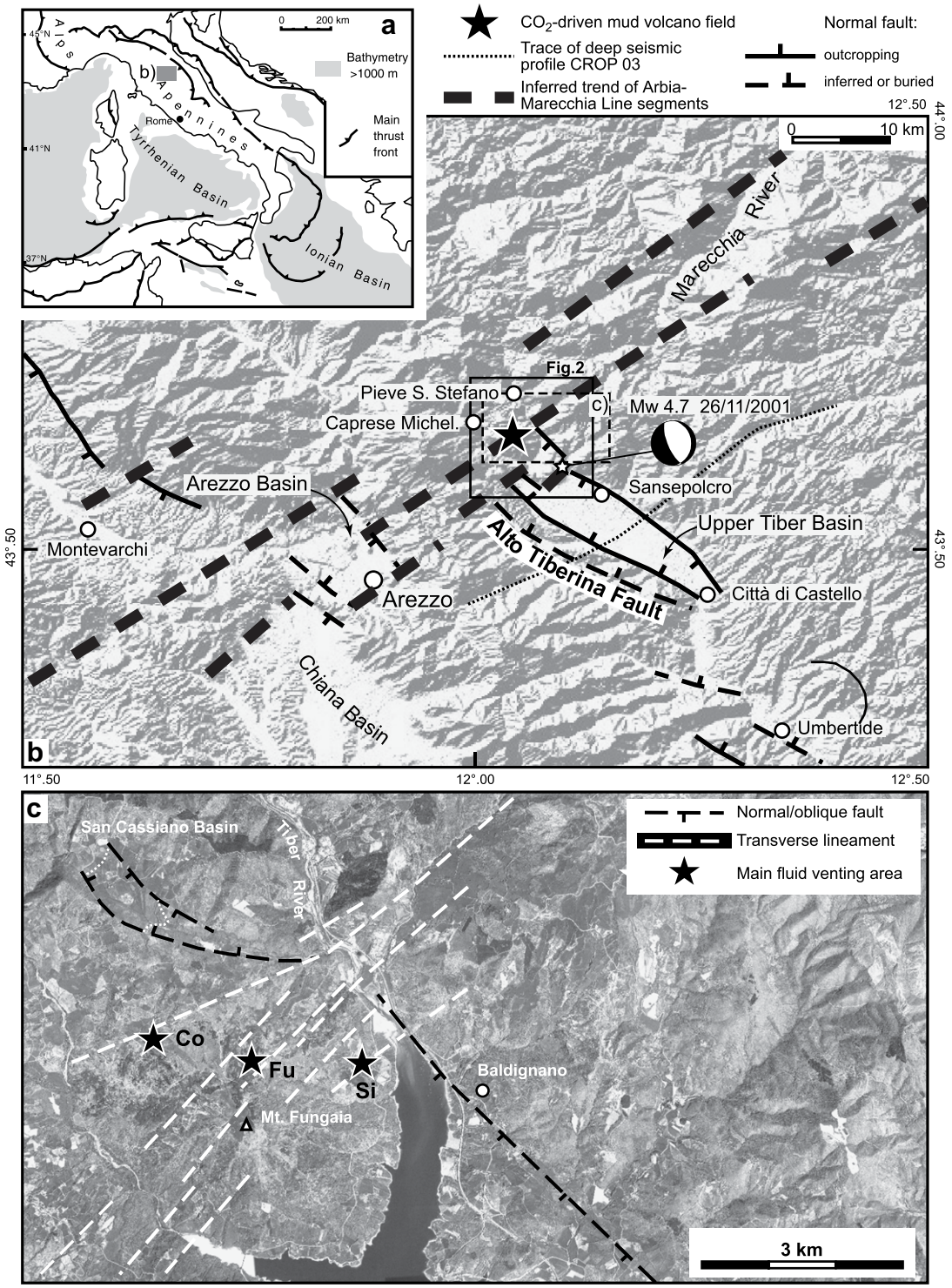

Fig. 1. (a) Location map, and (b) structural framework of the study area in Northern Apennines (Upper Tiber River). The main structural elements are plotted onto a digital shaded-relief elevation model (USGS, Shuttle Radar Topography Mission, hole-filled seamless SRTM data V1, 2004, CIAT, available from: http://gisweb.ciat.cgiar.org/sig/90m_data_tropics.htm), including the epicentre of earthquake of 26 November 2001 (43°36.00N, 12°06.52E; Castello et al., 2006). (c) Aerial photo showing the location of the main fluid venting areas (Co, Covivoli; Fu, Mt. Fungaia; Si, Sigliano) in relation to faults identified through analysis of aerial stereo photos and surveyed in the field.

general issue of structural controls on permeability patterns at the upper crustal levels (i.e., <5 km depth).

The present study concerns: (1) a detailed analysis of the surface fault pattern and its relations with surface venting; (2) the relations among fluid pressure regimes, rheological stratification of the substratum, and failure mechanisms along faults/fractures, which may potentially provide the fluid corridors; and (3) distribution of microseismicity that followed the earthquake of 26 November 2001.

2. Geologic framework

The NE-verging Northern Apennines fold-and-thrust belt developed as a consequence of Cenozoic collision between the Corso–Sardinian block and the Adriatic plate (e.g. Boccaletti and Guazzone, 1974; Principi and Treves, 1984). The Ligurian Units-allochthonous terrains scraped off from Alpine Tethys oceanic crust-correspond to the uppermost tectonic units in the Apennine nappe

pile. These units were thrust from west to east over the developing thrust wedge, which progressively incorporated tectonic units deposited as Miocene siliciclastic turbidite sequences in the Adriatic foredeep (Ricci Lucchi, 1986). Consequently, the Ligurian Units are tectonically superposed onto the Miocene turbidites, which, in the study area, are represented by the Falterona Sandstones.

The study area includes the Quaternary Upper Tiber Basin, which represents an area of active subsidence a few kilometres southeast of the mud volcano field (Fig. 1a). Analysis of geomorphic traces of recent faulting along the Upper Tiber Basin margins and earthquake fault plane solutions suggest that the normal faults bounding the basin are potentially seismogenic (Tanini, 1998; Delle Donne at al., 2007; Fig. 1). The recent seismic event of 26 November 2001 (Mw 4.7) occurred at the north-western margin of this basin and showed a nearly pure extensional faulting mechanism (INGV, 2001) compatible with the geometry of the NW-trending Alto Tiberina Fault (Heinicke et al., 2006) (Fig. 1a). This fault is visible in outcrop (Cattuto et al., 1995; Tanini, 1998), and it has been well imaged in various interpretations of the deep seismic profile CROP 03 crossing this basin (Barchi et al., 1998; Boncio et al., 2000; Finetti et al., 2001; Fig. 1b), as well as in shallow seismic profiles (Delle Donne et al., 2007).

The Upper Tiber Basin is clearly bounded to the northwest by a NE-trending fault system associated with the regional transverse tectonic lineament referred to as the "Arbia-Val Marecchia Line" (AVML), which is one of the various tectonic elements crossing transversely the whole Northern Apennines. These lineaments are normally interpreted as large and diffuse deformation zones composed of more fault segments, which may represent the surface response of old deep-seated faults active (with dominant strike-slip components) during the mountain building (e.g., Bortolotti, 1966; Boccaletti et al., 1977; Fazzini and Gelmini, 1982; Sorgi et al., 1998). According to some models, the south western segment of these structures was reactivated in extension and acted as transfer faults bounding the Late Miocene–Quaternary hinterland basins (Liotta, 1991, and references therein). Whereas the Alto Tiberina Fault has been documented to be an active structure, no obvious evidence for surface faulting and/or ongoing activity has been reported hitherto for the AVML, at least in the study sector. Activity of structures associated with this lineament can be only loosely referred to Quaternary times considering that they delimit some Quaternary sedimentary basins (Arezzo and Upper Tiber basins; Fig. 1b).

3. The Pieve Santo Stefano mud volcano field

3.1. Characteristics of venting

The Pieve Santo Stefano mud volcano field consists of active vents (locally known as *mofette* or *putizze*) clustered into three areas distributed on the northern flank of Mt. Fungaia, which is part of a large slab of Ligurian Units (Fig. 2). These areas are referred to hereinafter as Covivoli, Mt. Fungaia and Sigliano (Figs. 1c and 2). The evolution with time of morphologic characteristics of the Covivoli vents is described in detail in Heinicke et al. (2006). The surface vents consist of sub-circular craters mostly filled with turbulent bubbling muddy water owing to the vigorous expulsion of gases, which may reach hundreds of litres per minute. From a morphological point of view, the vents can be referred to muddy pools (Fig. 3a,b,e), and mud volcanoes when the presence of extrusive mud gives rise to small conic edifices (Fig. 3c). Generally, the mud extrusive features exhibit low topographic relief, and can be better described as "mud pie"-type mud volcanoes (slope angle $<5^\circ$; e.g., Kopf, 2002). However, morphologies referable to genuine mud volcanoes have been documented during the evolution of the vents, notably the conic-shape edifices (at Covivoli) resulting from the mud extrusion that occurred 18 months after the 2001 main shock. The extrusive mud and increased fluid flow have been interpreted as the propagation to the surface of a strong fluid pulse generated by the 2001 seismic sequence (Heinicke et al., 2006).

At the surface, the expelled fluids are characterised by the following composition (for complete analyses, see Vaselli et al., 1997), Covivoli: $CO_2 = 94.73\%$, $N_2 = 4.76\%$, $CH_4 = 0.44\%$, $H_2S = 0.04\%$, Ar = 18 ppm, $H_2 = 226$ ppm, He = 49.6 ppm; Mt. Fungaia: $CO_2 = 95.70\%$, $N_2 = 4.19\%$, $CH_4 = 0.07\%$, $H_2S = 0.02\%$, Ar = 32 ppm, $H_2 = 214$ ppm, He = 35.5 ppm. Unlike the Umbria–Marche region where CO_2 mostly results from mantle degassing (e.g., Chiodini et al., 2000), helium isotopes ($^3He/^4He$) ratios at the Pieve Santo Stefano vents indicate a crustal origin (Vaselli et al., 1997).

3.2. Structural analysis

To determine the relations between faults and surface venting, the structural pattern was analysed on a sufficiently broad area encompassing the northern part of the Upper Tiber Basin and a large segment of the AVML (Fig. 1b). The main structures were identified by integrating new field observations with analyses of aerial stereo photos and satellite imagery, as well as with the results of recent geological mapping (Regione Toscana, 2002–2005).

Previous studies suggest that fluid flow feeding mud volcanoes has been occurring along a segment of the NW-trending Alto Tiberina Fault. However, the CO_2-rich vents essentially coincide with the NE-trending faults cutting across the Mt. Fungaia area, and the NW-trending normal fault system bounding the Upper Tiber Basin apparently terminates against the main NE-trending AVML faults (Figs. 1c and 2). No unambiguous evidence for the existence of NW-trending normal faults has been identified to the north-west of this transverse fault zone. Interestingly, the 2001 seismic sequence localised at the northernmost (NW-trending) fault segment, outside the main depression, near the junction with the NE-trending fault set (Figs. 1 and 2).

In order to constrain the kinematics of main faults, fault-slip data were collected at selected sites of measurement. Slickensides measured on mesoscopic fault planes associated with the main faults bounding the Upper Tiber Basin revealed an essentially dip-slip kinematics (see the following Section 4.2). The analysis of faults associated with the AVML indicates instead a more complex kinematics, in which right-lateral movements predominate. Mesoscopic deformations associated with this fault zone mainly consist of NE–ENE-striking right-lateral faults with both transtensional and transpressional component. The right-lateral faults are often found to dislocate previous gently dipping thrusts. The dextral component of displacement is manifested by both fault-slip data collected along the main faults (sites 1–3 and 5–8; Fig. 2) and by the consistent offset undergone by lithological or tectonic contacts along NE-trending faults (Fig. 2). Such a dextral offset of geological units is particularly evident east of Mt. Fungaia (Sigliano), and south of the Viamaggio Pass (Fig. 2).

The relations with active venting are well expressed near Covivoli, where three vents are clearly aligned in a ca. N50°E direction that strikingly parallels to the surrounding AVML-related transverse faults (Fig. 3d). Analysis of mesoscopic structures collected near the venting area, along the trace of a major NE-trending fault, has revealed the presence of a consistent right-lateral fault kinematics (site 5 in Figs. 2 and 3d). In addition, a N50°E–N70°E-striking set of fractures has been identified in the vicinity ($\leq$5–10 m) of the active vents (see inset in Fig. 3f). Interestingly, such fractures displace the ground with a vertical offset up to 0.5 m, and can be traced for a length of ca. 150 m. The parallelism of such a fault/fracture set with the alignment(s) defined by individual vents (Fig. 3d,f) suggests this set to be intimately associated with the emission of fluids to the surface. These fractures presumably reflect a deeper structure controlling the location of a shallow fluid

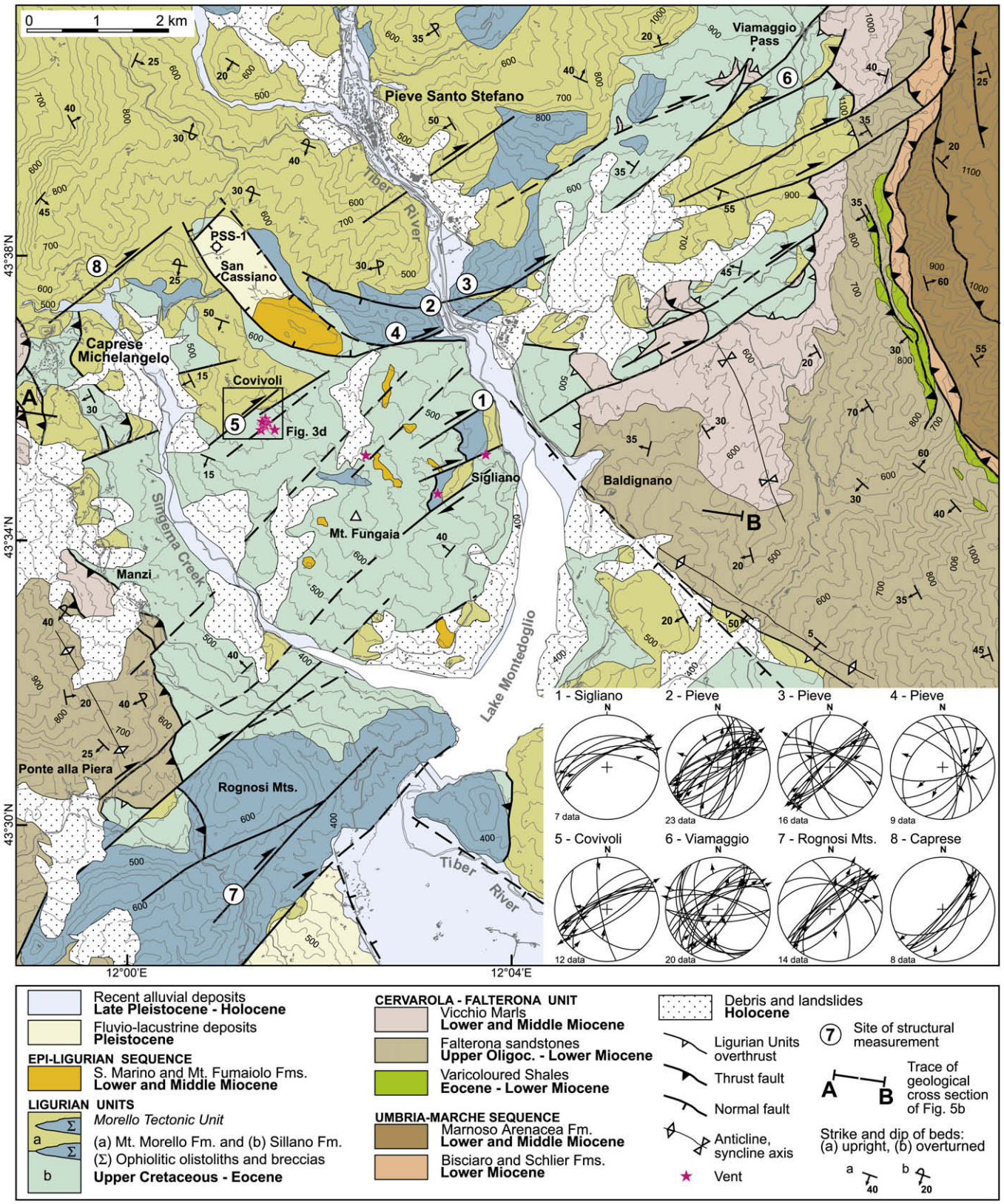

Fig. 2. Tectonic and geological sketch map of the vents area, between Caprese Michelangelo and Pieve Santo Stefano (adapted from Regione Toscana, 2002–2005). The stereonets indicate fault-slip data collected at selected sites of measurements (1–8) along the main transverse faults (Wulff net, lower hemisphere). Contour lines are 50 m apart.

reservoir, and most probably they developed to accommodate the collapse ensuing fluid expulsion.

Hints about the timing of deformation of the transverse fault system are provided by the analysis of the small San Cassiano Basin, located ~2 km north of the Covivoli vents (Figs. 1c and 2). This basin is mostly filled by continental silts, sands, and subordinately gravels, loosely attributed to the Pleistocene (Carta Geologica d'Italia, 1969; Anelli et al., 1994). The San Cassiano Basin is

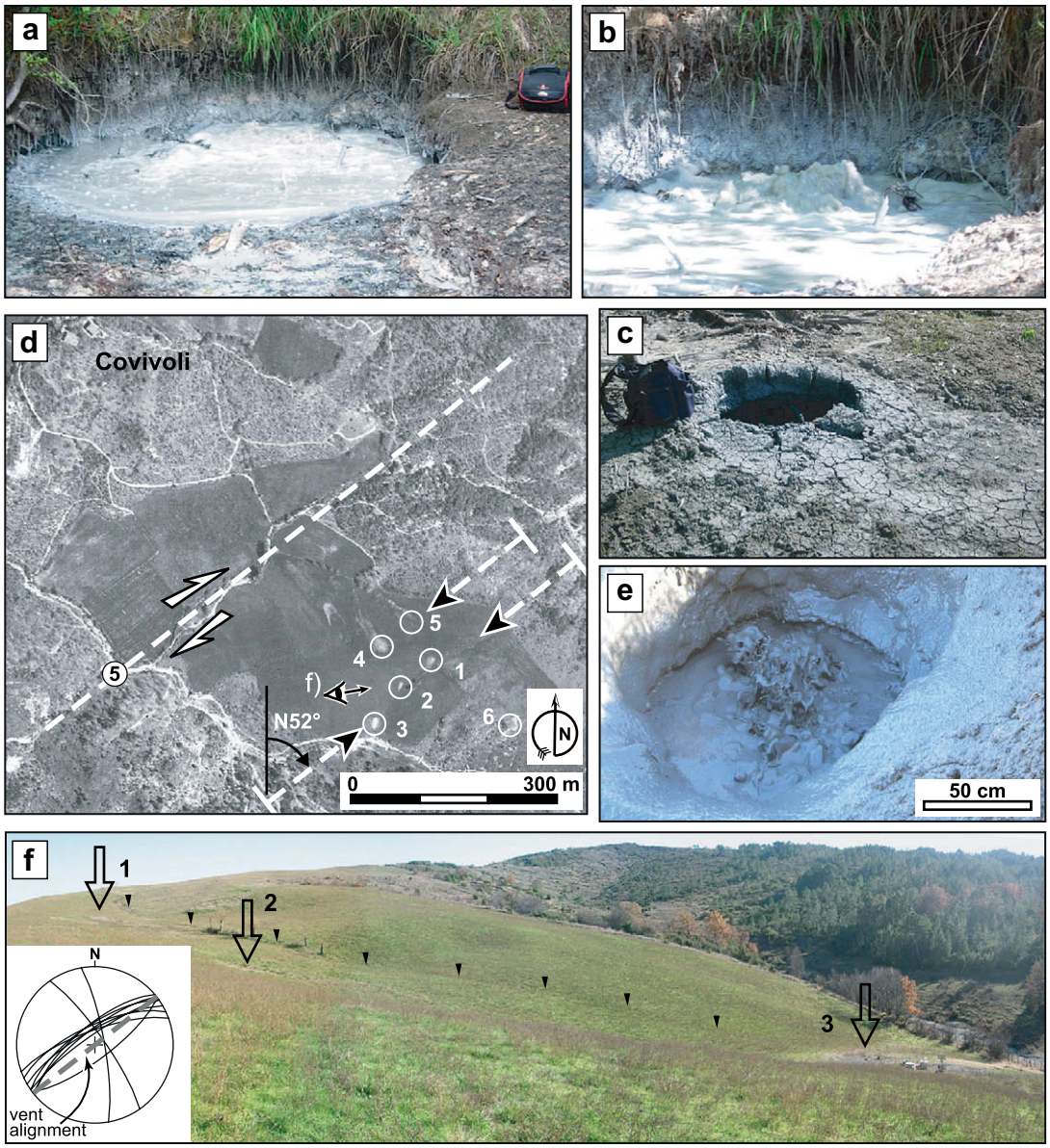

Fig. 3. Carbon dioxide dominated surface venting in the Caprese Michelangelo–Pieve Santo Stefano area. Mt. Fungaia vent: (a) Mud pool filled with bubbling muddy water owing to the elevated gas flux, and (b) close-up of the turbulent bubbling of water. (c) Mud pie-type mud volcano built by extrusive mud accompanying gas expulsion. (a) June 2007, (b) and (c) May 2007. Covivoli vent: (d) Aerial photograph showing the location of main vents 1–6 (encircled) and of a dextral fault (dashed) identified through analysis of aerial stereo photos and surveyed in the field (structural site 5); blackhead arrows point to vent alignment. (e) Turbulent flow of muddy water at vent 4. (f) Alignment of vents 1–3 (indicated by open arrows); photo point of view in (d). The plot in the inset (Wulff net, lower hemisphere) reports the orientation of fractures and cracks (denoted by the tip of black triangles) displacing the ground; (e) and (f) November 2007.

topographically higher than the Upper Tiber Basin, and is bounded at the southwestern margin by a ~NW–SE-trending main normal fault that gradually connects to NE-trending dextral faults of the AVML (Fig. 2). On this basis, the San Cassiano Basin can be genetically interpreted as "horsetail splay" depression forming at the southwestern tip of a NE-trending dextral fault (e.g., Biddle and Christie-Blick, 1985). This correlation gets further support to the inferred Quaternary activity of the AVML faults.

3.3. Structure of substratum and characteristics of trapped fluids

The deep PSS-1 well for hydrocarbon exploration (4936 m total depth), located in the San Cassiano Basin, gives a valuable indication about the structure of the vents' substratum (Anelli et al., 1994; Fig. 2). Below 66 m of continental deposits, the well drilled ca. 800 m of Ligurian Units rocks dominated by limestones, sandstones and marls (Monte Morello Fm.), and subordinately by limestones and shales (Sillano Fm.). However, surface geology suggests the Ligurian Units beneath the main vents should consist of shales and limestones of the Sillano Formation (see Fig. 2). Below the Ligurian Units, the PSS-1 well encountered the Miocene Falterona Sandstones (up to 1853 m), and then Umbria–Marche carbonate rocks up to 3152 m depth. From 3295 to 4936 m depth, the vertical rock column consists of an alternation of tectonic slices composed of Oligocene–Miocene volcanics (andesites) and Triassic anhydrites and dolostones (Burano Fm.).

A relevant fraction of carbon dioxide is found at a depth of 3700 m, presumably at the top of the main fluid reservoir, under a pressure of 700 bars (=70 MPa), 120 °C, and density 860 kg m^{-3} that points to supercritical fluid states (Heinicke et al., 2006). These physical fluid conditions postdate both the 2001 seismic sequence and the time the fluid pressure wave reached the Covivoli vents.

The main fluid reservoir resides into the Burano Fm. (made of evaporites and dolostones), which acts as a sealing barrier to fluid generated into the deeper levels. The chemical composition of the trapped fluid was $CO_2 = 92.2\%$, $N_2 = 7.6\%$, $CH_4 = 0.03\%$, $O_2 = 0.01\%$, $H_2S < 0.02\%$, $H_2O < 0.5\%$. Comparison with surface gas composition (see Section 3.1) suggests methane (CH_4) to be generated in the rock column overlying the reservoir, most likely in the Falterona sandstones.

The level of pore fluid pressure (P_f) can be expressed by the factor λ_v, which is the ratio of P_f to vertical (lithostatic) stress, ρgz (Hubbert and Rubey, 1959). Pore fluid factors $\lambda_v = 0.4$ and $\lambda_v = 1$ denote hydrostatic and lithostatic states, respectively. In the fluid reservoir encountered by the PSS-1 well, factor λ_v was approximately 0.75 (considering $P_f = 70$ MPa, $\rho \approx 2600$ kg m^{-3}), which corresponds to a rather elevated overpressure. Similar λ_v values can be assumed to characterise the post-seismic conditions in the fluid reservoir beneath our fluid vents.

4. Discussion

4.1. Vertical fluid migration and fluid pressure states at depth

Studies of mud volcanoes and their related features provide useful windows into how fluids move through the shallow crust. Surface venting at Pieve Santo Stefano is in fact controlled by brittle elements linked to a deep-seated fluid reservoir, and shows relations with nearby seismicity. The post-seismic anomalous increase in fluid flux recorded at such mud-volcano sites likely manifested the propagation to the surface of a fluid pressure front originated from the coseismic rupture of a fault segment at depth (Heinicke et al., 2006). Obviously, the transfer of deep fluids to the surface vents depends upon the presence of open pathways, presumably represented by zones of fractures or faults, extending downward to reach the deep reservoir. The correlation between vent/fracture distribution and fault trend suggest that fluid emission occurred along the steep AVML transverse faults (Fig. 3d,f), which are thus inferred to represent efficient and permeable conduits channelling fluids to the surface.

In this process, the vertical superposition of rock packages with different permeability, as revealed by PSS-1 well stratigraphy, may strongly influence the local fluid pressure state. Particularly, the occurrence of impermeable macro-layers is a favourable condition for trapping fluids and pore fluid pressure built-up, and is thereby able to play a relevant role in the process (e.g., Hunt, 1990; Neuzil, 1995). At the same time, cemented faults or fractures may form sealing barriers to fluid migration, or serve as cross-stratal conduits for large fluid flow if they are permeable structures. The presence of CO_2-rich fluids introduces more complexity to the process, as fault healing in carbonate rocks is also strongly dependent upon partial pressure of CO_2 (see the following Section 4.3).

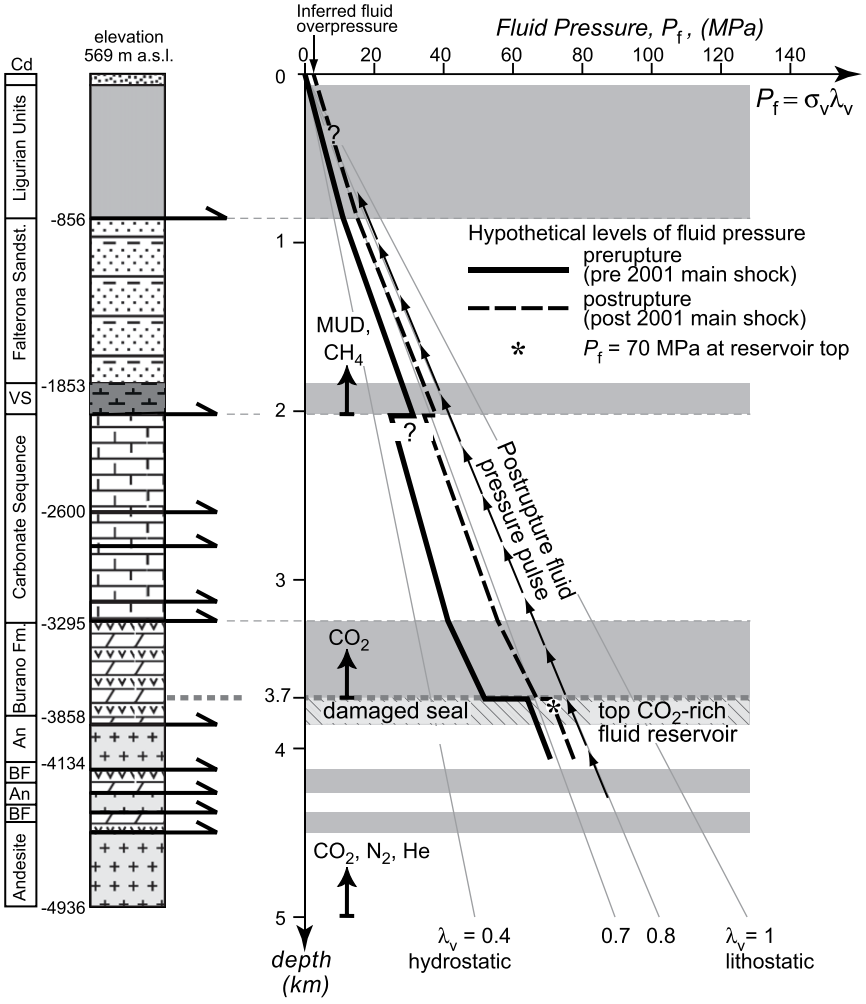

Fig. 4. Schematic cartoon showing fluid pressure variations with the depth matched with the stratigraphy of well "Pieve Santo Stefano 1" (PSS-1; simplified from Anelli et al., 1994), which can be taken as representative of the mud volcano area. Grey shading indicates potential sealing barriers pointing to a multiple seal setting. The magnitude $\lambda_v \approx 0.75$ refers to conditions postdating the 2001 seismic crises. An, andesites (Oligocene–Miocene); BF, Burano Formation (Triassic); VS, Varicoloured Shales (Middle–Upper Eocene); Cd, San Cassiano Pleistocene continental deposits (Pleistocene).

The relations between fluid pressure states and vertical rheological stratification in the study vents are illustrated in a speculative fluid pressure/depth diagram (Fig. 4). The strong gas flux and turbulent bubbling observed at the vents (e.g. Fig. 3a,b,e) suggests a rather high fluid pressure up to the surface where values well above hydrostatic ($\lambda_v \gg 0.4$) can be inferred (Fig. 4). The relative impermeable (and "plastic") Ligurian Units (mostly shales and limestones) and Burano Fm. (evaporites and dolostones) most likely represent the main barriers to fluid migration at depth. The observation that the top of the deep overpressured main fluid reservoir resides in the Burano Fm. suggests that the lower part of this seal is permeable, possibly because it was damaged by hydraulic fracturing developing during overpressured, or even supralithostatic, fluid regimes (Fig. 4; e.g., Foxford et al., 2000).

High CO_2 pressure would assist flow up through the carbonate succession above the seal reservoir (Burano Fm.) by imparting an undersatured character to the raising fluid that helps maintaining the fluid pathways open (Fig. 4). An increase in P_f may be expected within the overlying Falterona sandstones, which should be less sensitive to the erosion operated by CO_2-rich fluids. However, the occurrence of gas emissions before the 2001 seismic event unequivocally manifests the presence of steep permeable faults or fractures. The transition from pre-seismic dominantly gaseous manifestations (Vaselli et al., 1997) to post-seismic occurrence of extrusive mud (in addition to gases) reveals an obvious change in the characteristics of fluid expulsion. Specifically, the absence of mud and the limited presence of H_2O in the reservoir ($H_2O < 0.5\%$) suggest the source layer of mud to reside into the Falterona sandstones (or neighbouring shale units) where the presence of formation water may have fluidised the mud during the passage of the seismically induced fluid pressure pulse (Fig. 4). Pore fluid pressure built-up related to the presence of the impermeable Ligurian Units over the Falterona Sandstones may have sustained the process too.

4.2. Relations with local seismicity

The main seismic shock of 26 November 2001 occurred at a depth of 10 km (INGV, 2001) and was characterised by an aftershock sequence with hypocentres located at depths varying between ca. 2 and 7 km (Castello et al., 2006). Analysis of hypocentral depths suggests such a seismic crisis migrated upward along a fault plane dipping 35° to the NE, corelatable to the Alto Tiberina Fault. The general swallowing trend of events with time suggests that some of these microearthquakes could be linked to the transport of fluids toward the surface vents (Heinicke et al., 2006). An intimate link between aftershock generation and fluid pulses generated by post-seismic degassing of trapped high-pressure CO_2-rich fluid sources has also been documented for the 1997 Umbria–Marche seismic sequence, located 100 km southeast of the study area (Miller et al., 2004). In this model, the pressure pulse propagating from the damage zone created during the main earthquake propagated according to the hydraulic connectivity, and triggered aftershocks by significantly reducing the effective confining stress.

In the same way, a preliminary analysis of the time-space distribution of seismicity suggests that, after the main events of November 2001, seismicity in the Upper Tiber Basin area migrated (December 2001) along strike the normal faults trend, and then localised along the transverse AVML faults (Fig. 5a,b). This evolution accords well with the strong subhorizontal σ_2 permeability expected in normal fault systems as a consequence of along-strike hydraulic communication (Sibson, 2000). Accordingly, analysis of fault-slip data collected on the faults delimiting the Upper Tiber Basin reveals a mean NE-directed extension (σ_3 axis) and a ca. NW-oriented σ_2 axis, which trend orthogonal and parallel to the normal faults, respectively (Fig. 5a).

Different mechanisms may account for the microearthquakes along the NW–SE fault trend: (1) reactivation of Upper Tiber Basin normal faults; (2) rupture of new "Andersonian" faults; and (3) hydraulic fracturing, in which tension fractures form orthogonal to the σ_3 axis when $P_f > \sigma_3 + T$ (where T is the tensile strength of rock). The use of a Mohr diagram (with a Griffith–Coulomb failure envelop) may help discriminating between these failure modes. The relations between fault trend and orientation of the stresses obtained from the inversion methods (Fig. 5a) allow the application of reshear theory (Sibson, 1985) to the NW–SE-trending faults. For a cohesionless normal fault containing the σ_2 axis at an angle θ_r to the σ_1 direction (in this case vertical), the reshear conditions may be written in terms of differential stress and minimum effective principal stress (Sibson, 2000):

$$(\sigma_1 - \sigma_3) = \frac{\mu_s(\tan\theta_r + \cot\theta_r)}{(1 + \mu_s \cot\theta_r)} \rho g z (1 - \lambda_v), \quad (1)$$

$$\sigma'_3 = (\sigma_3 - P_f) = \frac{(1 - \mu_s \tan\theta_r)}{(1 + \mu_s \cot\theta_r)} \rho g z (1 - \lambda_v). \quad (2)$$

The fault reactivation conditions may be evaluated by plotting Eqs. (1) and (2) on the Griffith–Coulomb diagram taking into account the parameters specific for the considered case. In the study area, the reactivation angle θ_r is approximately 40° (the complement to the average dip, ca. 50°, of normal faults bounding the Upper Tiber Basin; see stereonet in Fig. 5a), while a depth $z = 5000$ m is taken as an average hypocentral depth of microseismicity of 2001 seismic crises. Various cases are represented (assuming $\rho = 2600$ kg m^3, $\mu_s = 0.6$, $T = 10$ MPa) in relations to fluid pressure states (Fig. 6). From the analysis of the different P_f and differential stress states, at the considered depth, the plane $2\theta_r = 80°$ is favourably oriented for frictional reactivation for a large variety of P_f and differential stresses, as reshear may occur even at hydrostatic regimes (Fig. 6). Therefore, this state tends to prevent attainment of the tensile overpressure condition ($P_f > \sigma_3$, or $\sigma'_3 < 0$) required for hydraulic extension fracturing and extensional-shear failure.

However, other parameters may greatly influence this process and affect the above considerations, such as the coefficient of frictional reactivation, μ_s, and tensile strength, T. The magnitude of μ_s may play a very important role in the mechanics of low-angle faulting (Collettini and Holdsworth, 2004). Most notable for the case under study may be the magnitude of tensile strength. Typical T values for intact sedimentary rocks vary between 1 and 10 MPa, while T may exceed 20 MPa in crystalline rocks (Lockner, 1995). Tensile strength of fault and fracture planes, T_F, is expected to fall in the lower range of sedimentary rocks, but the occurrence of sealing and cementation may increase these values considerably. In addition, T_F may strongly vary with time during the fault failure cycle. The relevance of T to this process is exemplified by considering lower tensile strengths. For $T = 5$ MPa, both a relevant fluid pressure ($\lambda_v > 0.7$) and a relatively small differential stress (ca. <40 MPa) are needed for frictional reactivation, as a new "Andersonian" fault will develop at lower fluid pressure regimes (Fig. 6). For $T = 2$ MPa more extreme pore fluid pressure regimes ($\lambda_v > 0.85$) and lower differential stresses (ca. <18 MPa) are required in order for frictional reactivation to occur (Fig. 6). Unfortunately, no direct measurements of T (or T_F) are available in the area, but the occurrence in the study area of relevant overpressures ($\lambda_v \approx 0.75$) may suggest frictional reactivation along favourably oriented planes to be the most favourable mechanism creating the post-seismic microseismicity in the NW–SE direction (Fig. 5a).

Very much reduced tensile strengths along the NE-trending faults/fractures may be potentially responsible for their preferential

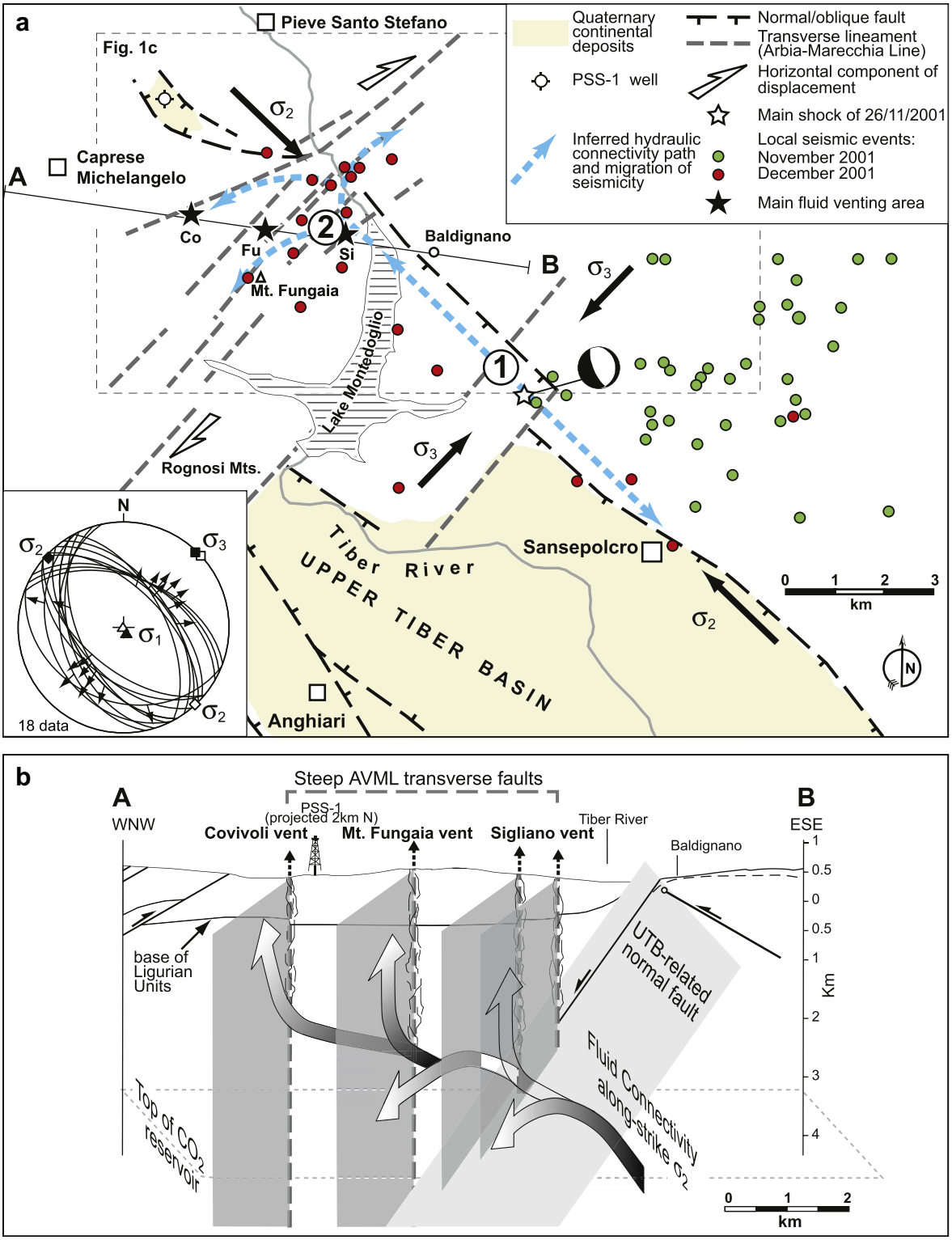

Fig. 5. (a) Inferred relations between tectonic structures and time-space distribution of microseismicity following the main shock of 26 November 2001 (seismicity from Heinicke et al., 2006). December 2001 microseismicity is inferred to have migrated (1) along-strike σ_2 (i.e., in a NW–SE direction), and then (2) along NE-trending permeable pathways provided by pre-existing steep transverse faults. The plot shown in the inset (Wulff net, lower hemisphere) reports the cumulative mesoscopic faults collected along the trace of active faults bounding the Upper Tiber Basin, and is thus deduced to reflect the Holocene stress field. This latter has been computed through dihedron angles (Angelier and Mechler, 1977) and P & T axes (e.g., Caputo and Caputo, 1988) inversion methods, which are denoted by white and black ornaments, respectively. (b) Conceptual 3D model showing hydraulic connectivity associated with the main structures in the area, specifically the NW–SE-trending Upper Tiber Basin normal faults and the steep AVML faults pre-existing the development of the basin. Fluid flow along the transverse faults is expected to occur into the associated damage zones, which may be longitudinally interconnected by both pre-existing thrust faults and newly formed normal fault segments. The trace of the geological cross section is also reported in Fig. 2. UTB, Upper Tiber Basin.

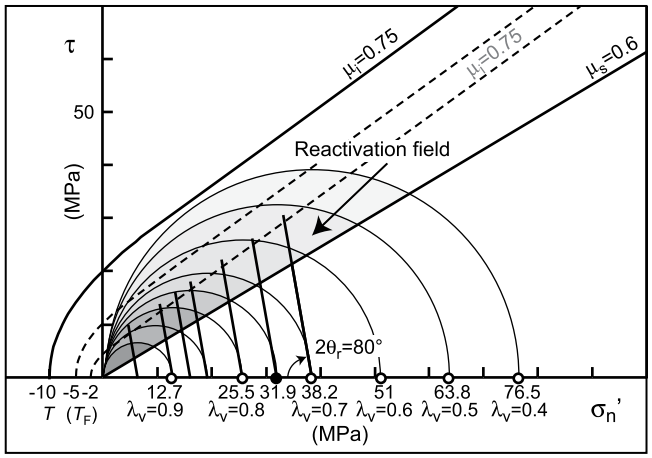

Fig. 6. Composite Griffith–Coulomb failure envelope for intact rock ($\mu_i = 0.75$), and fault reactivation conditions in anisotropic rocks ($\mu_s = 0.6$). Differential stress required for frictional reactivation ($z = 5000$ m; $\mu_s = 0.6$; $\rho = 2600$ kg m^{-3}; $T = 10$ MPa) of a normal fault plane dipping 50° ($2\theta_r = 80°$) in relation to fluid pressure P_f. The black dot indicates the fluid pressure conditions ($\lambda_v = 0.75$) measured in the area. The 50°-dipping fault plane is favourably oriented for reactivation in suprahydrostatic regimes for $T = 10$ MPa. Higher fluid pressure and lower differential stresses are needed for lower T values. Grey shadings indicate the reactivation field(s).

opening, and the consequent development of the pathways allowing the observed fluid seepage. Similar results may be obtained if $\sigma_2 = \sigma_3$, which implies the stress ratio $\phi = (\sigma_2 - \sigma_3)/(\sigma_1 - \sigma_3) = 0$. Under these special conditions, some extension fractures may occur in NE directions and their trace on the NE-trending fault planes can make angles from 0° to 90° with the direction of maximum resolved shear stress (see Blenkinsop, 2008).

Concerning the microearthquakes localising on these transverse faults, a frictional reactivation of such structures as transfer faults accommodating the slip along the NW–SE-trending faults is kinematically admissible, but no evidence for active faulting has been documented for these features so far. Therefore, the post-seismic increased fluid flow and the relevant overpressures at well PSS-1 are taken as evidence for the potential role of hydraulic fracturing as the triggering process for the seismicity along the transverse structures. Particularly, the post-seismic fluid pressure wave (along the way to the surface vents) may have triggered the explosion of pressurised fluid pockets, trapped into the damage zone of transverse faults, by locally increasing the fluid pressure to exceed $\sigma_3 + T$. Since hydraulic extension fractures form orthogonal to the σ_3 ($2\theta_r = 0°$), in the assumed regional stress field of Fig. 5a the fluid pockets are expected to have opened roughly parallel to the transverse faults trend.

Finally, it is worth noting that both the pre-seismic and post-seismic raising of fluids up-through the NE-trending steep permeable faults is favoured by the steepness of these brittle elements, which can be estimated to be ≥70° (Fig. 5b). The process may be conceptually similar to the intrusion of magma into existing fractures or faults, in which the pressure required to penetrate these elements decreases with increasing their steepness (i.e., with the decreasing of normal stress acting on the fault plane) (Jaeger and Cook, 1976; Acocella et al., 1999). Accordingly, no post-seismic surface fluid discharge has been reported to occur along the NW-trending normal faults, which show an obvious gentler dip than the steep faults associated with the strike-slip dominated AVML.

4.3. Relevance of CO_2-rich fluids to fault-valve action

Fluid forcing on fault failure events described in terms of fault-valve activity has received increasing support (Ramsay, 1980; Sibson, 1992, 2007; Byerlee, 1993; Hickman et al., 1995; Petit et al., 1999). More specifically, fault-valve behaviour is a cyclic process in which fluids trapped in overpressured compartments are released intermittently through a ruptured fault as pore fluid pressure has risen enough to weaken the fault under stress loading. Fluid expulsion contemporaneous to fault failure will result in the drop of pore fluid pressure internal to the ruptured fault. The following effective stress increase will promote fault sealing, which will in turn lead to a renewed accumulation of fluid overpressure and a decrease of fault strength. This intriguing process has been applied to various natural cases (Sibson, 1981, 1992; Cox, 1995), and could explain the surface fluid expulsion accompanying seismic events (e.g., Sibson, 2007). Severe fault valving is expected to occur along steep reverse faults under a compressional regime (Sibson, 1992), but this process may also develop in normal fault systems

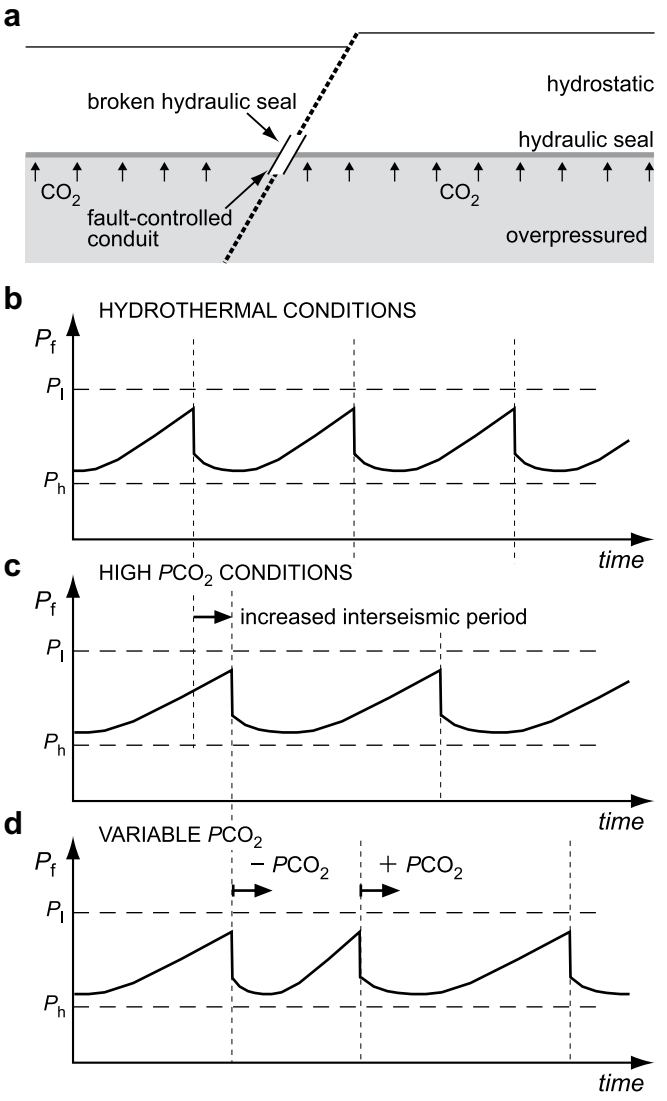

Fig. 7. Influence of CO_2-rich fluids circulating in carbonate rocks on a fault failure cycle controlled by fault valving behaviour, which is schematically illustrated in fluid pressure (P_f)-time diagrams (both tectonic load and stress drop at failure are constant). (a) Fault transecting a large thickness of carbonate rocks (such as in the study area) including a hydraulic seal separating an overpressured compartment from an overlying compartment in hydrostatic regime. (b) Conceptual fault failure cycle in the case of silica-rich fluids (a and b are inspired from Sibson, 2000). (c) The presence of pressurised CO_2-rich fluids may potentially increase (in comparison with b) the recurrence interval between successive faulting events. (d) Decrease or increase in partial pressure of CO_2 (PCO_2) subsequently fault failure may strongly condition fault sealing and affect the fault failure cycling. P_h and P_l, hydrostatic and lithostatic fluid pressure, respectively.

(Sibson, 2000). An example of this is the post-seismic fluid pressure wave generating the aftershock sequence of the 1997 Umbria–Marche earthquake (Miller et al., 2004), recorded by variations in CO_2 release at the surface (Caracausi et al., 2005). Similar considerations can be made for the post-seismic fluid discharge and mud extrusion described for the study vents, which may also represent an episode of fault-valve behaviour occurring in the shallow crust.

However, the recurrence interval between successive faulting events is a complex process basically controlled by the renewal of fluid pressure following fault-fracture resealing, and by shear stress build-up, which in turn depends upon a number of factors, like rupture permeability and the resealing rate (Sibson, 1992). The presence of CO_2-rich fluids circulating in carbonate rocks may introduce more complexity to the process. The observation that surface venting in the study area was occurring also before the 2001 seismic crises implies that the fluid pathways were not cemented but connected to the deep reservoir. Though no slip is inferred to have taken place on these transverse structures, their evolution may suggest some implications for the fluid–fault interactions at the NW-trending normal faults. CO_2-rich fluids may indeed play a relevant role in this process, seeing that fluids with high partial pressure of CO_2 (PCO_2) are undersatured and tend to dissolve rather than precipitate. In these circumstances, fluid pressure recovery within the created damage fault zone may be significantly slow, so that post-failure fault/fracture healing (and consequent decrease in fault permeability and increase in fault strength) in carbonate rocks may take a longer time than when other fluids are present, for instance hydrothermal precipitation of silica-rich fluids. An obvious implication is that, by influencing the resealing rate and fluid pressure recovery, high PCO_2 fluids circulating in carbonate rocks may affect the fault failure cycling by comparatively increasing the interseismic period in the theoretical case in which shear stress accumulation stays constant (Fig. 7b,c).

Additionally, variations of factors such as: (1) porosity and/or permeability of rocks surrounding the fault; (2) temperature; (3) pH; and (4) concentration of carbonate in mineral waters, may all induce variations of PCO_2, which may move the fluid toward either saturated (precipitation) or undersaturated (aggressive) solutions. As a result, the consideration that relevant variations in PCO_2 may be expected during the fault-failure cycle -such as after the modifications induced by fault failure- introduces further complexity to the process. For example, an increase or a decrease of PCO_2 is expected to postdate or predate the next faulting event, respectively (Fig. 7d). These variations may thus largely affect fault-slip recurrence intervals, thereby seismic hazard estimates, especially in areas with high CO_2 production like the Apennines.

5. Concluding remarks

(1) Integrated structural analyses have allowed establishing that the main venting centres at Pieve Santo Stefano are located along a transverse system of steep faults associated with the Arbia-Val Marecchia Line. These faults predate the Upper Tiber Basin occurrence, and show a dominant right-lateral kinematics that can be loosely ascribed to extend up to Quaternary times.

(2) Variation of fluid pressure with depth is controlled by a multiple seal system. The effect of the fluid pressure wave generated by the earthquake of 26 November 2001 superimposed onto this system, and induced a variation in the fluid emission style that in some cases passed from essentially gaseous to that typical of mud volcanoes. In this process, the pre-existing steep (NE-trending) transverse faults acted as permeable pathways that allowed the transport of overpressured fluids to the surface.

(3) Like other examples from the Apennines, the aftershock sequence was conditioned by the hydraulic connectivity, and propagated along the NW-trending normal faults bounding the Upper Tiber Basin, and then along the (NE-trending) transverse faults. Microseismicity along the former fault set is likely associated with frictional reactivation processes, whereas hydraulic fracturing is the most likely candidate for the microearthquakes along the transverse faults.

Acknowledgements

I'm grateful to Valerio Acocella and Tom Blenkinsop for thoughtful reviews and comments that significantly improved the original manuscript. The paper also benefited from the inspiring discussions with Angelo Minissale, Federico Sani, and Orlando Vaselli. Research supported by CNR-IGG ordinary funds.

References

Acocella, V., Salvini, F., Funiciello, R., Faccenna, C., 1999. The role of transfer structures on volcanic activity at Campi Flegrei (Southern Italy). Journal of Volcanology and Geothermal Research 91, 123–139.
Anelli, L., Gorza, M., Pieri, M., Riva, M., 1994. Subsurface well data in the Northern Apennines (Italy). Memorie Società Geologica Italiana 48, 461–471.
Angelier, J., Mechler, P., 1977. Sur une méthode graphique de recherche des contraines principales égalment utilisable en tectonique et en sismologie. Bulletin de la Société Géologique de France 19, 1309–1318.
Barchi, M.R., Minelli, G., Pialli, G., 1998. The CROP 03 profile: a synthesis of results on deep structures of the Northern Apennines. Memorie Società Geologica Italiana 52, 383–400.
Biddle, K.T., Christie-Blick, N., 1985. Glossary–Strike-slip deformation, basin formation, and sedimentation. In: Biddle, K.T., Christie-Blick, N. (Eds.), Strike-Slip Deformation, Basin Formation, and Sedimentation, vol. 37. Society of Economic Paleontologists and Mineralogists (SEPM) Special Publication, pp. 375–386.
Blenkinsop, T.G., 2008. Relationships between faults, extension fractures and veins, and stress. Journal of Structural Geology 30, 622–632, doi:10.1016/j.jsg.2008.01.008.
Boccaletti, M., Guazzone, G., 1974. Remnant arcs and marginal basins in the Cainozoic development of the Mediterranean. Nature 252, 18–21.
Boccaletti, M., Coli, M., Napoleone, G., 1977. Nuovi allineamenti strutturali da immagini Landsat e rapporti con l'attività sismica negli Appennini. Bollettino Società Geologica Italiana 96, 679–694.
Boncio, P., Brozzetti, F., Lavecchia, G., 2000. Architecture and seismotectonics of a low-angle fault in central Italy. Tectonics 19, 1038–1055.
Bortolotti, V., 1966. La Tettonica Trasversale Dell'Appennino. 1-La Linea Livorno-Sillaro. Bollettino Società Geologica Italiana 85, 529–540.
Byerlee, J.D., 1993. Model for episodic flow of high pressure water in fault zones before earthquakes. Geology 21, 303–306.
Caputo, M., Caputo, R., 1988. Structural analysis: new analytical approach and applications. Annales Tectonicae 2, 84–89.
Caracausi, A., Italiano, F., Martinelli, G., Paonita, A., Rizzo, A., 2005. Long-term geochemical monitoring and extensive/compressive phenomena: case study of the Umbria Region (Central Apennines, Italy). Annales Geophysicae 48, 43–53.
Carta Geologica d'Italia, 1969. Geological map, sheet n. 115 "Città di Castello", scale 1:100,000. Poligrafiche Bolis, Bergamo.
Castello, B., Selvaggi, G., Chiarabba, C., Amato, A., 2006. CSI Catalogo della sismicità italiana 1981–2002, versione 1.1. INGV-CNT, Roma. http://www.ingv.it/CSI/.
Cattuto, C., Concetti, C., Fisauli, M., Gregari, L., 1995. I bacini pleistocenici di Anghiari e Sansepolcro nell'alta valle del F. Tevere. Il Quaternario 8, 119–128.
Chiodini, G., Frondini, F., Cardellini, C., Parello, F., Peruzzi, L., 2000. Rate of diffuse carbon dioxide Earth degassing estimated from carbon balance of regional aquifers: the case of central Apennine, Italy. Journal of Geophysical Research 105, 8423–8434.
Collettini, C., Holdsworth, R.E., 2004. Fault zone weakening processes along low-angle normal faults: insights from the Zuccale Fault, Isle of Elba, Italy. Journal of the Geological Society of London 161, 1039–1051.
Cox, S.F., 1995. Faulting processes at high fluid pressures: an example of fault valve behavior from the Wattle Gully Fault, Victoria, Australia. Journal of Geophysical Research 100, 12,841–12,859.
Delle Donne, D., Piccardi, L., Odum, J.K., Stephenson, W.J., Williams, R.A., 2007. High-resolution shallow reflection seismic image and surface evidence of the Upper Tiber Basin active faults (Northern Apennines, Italy). Bollettino Società Geologica Italiana 126, 323–331.
Etiope, G., Feyzullayev, A., Baciu, C.L., Milkov, A.V., 2004. Methane emission from mud volcanoes in eastern Azerbaijan. Geology 32, 465–468.
Fazzini, P., Gelmini, R., 1982. Tettonica trasversale nell'Appennino Settentrionale. Memorie Società Geologica Italiana 24, 299–309.
Finetti, I., Boccaletti, M., Bonini, M., Del Ben, A., Geletti, R., Pipan, M., Sani, F., 2001. Crustal section based on CROP seismic data across the North Tyrrhenian-Northern Apennines-Adriatic Sea. Tectonophysics 343, 135–163.
Foxford, K.A., Nicholson, R., Polya, D.A., Hebblethwaite, R.P.B., 2000. Extensional failure and hydraulic valving at Minas da Panasqueira, Portugal: evidence from

vein spatial distributions, displacements and geometries. Journal of Structural Geology 22, 1065–1086.
Heinicke, J., Braun, T., Burgassi, P., Italiano, F., Martinelli, G., 2006. Gas flow anomalies in seismogenic zones in the Upper Tiber Valley, Central Italy. Geophysical Journal International 167, 794–806, doi:10.1111/j.1365-246X.2006.03134.x.
Hickman, S., Sibson, R., Bruhn, R., 1995. Introduction to special section: Mechanical involvement of fluids in faulting. Journal of Geophysical Research 100, 12,831–12,840.
Hubbert, M.K., Rubey, W.W., 1959. Role of fluid pressure in mechanics of overthrust faulting. Geological Society of America Bulletin 70, 115–166.
Hunt, J.M., 1990. Generation and migration of petroleum from abnormally pressured fluid compartments. AAPG Bulletin 74, 1–12.
INGV, 2001. http://legacy.ingv.it/~roma/reti/rms/terremoti/italia/arezzo/arezzo.html; http://legacy.ingv.it/seismoglo/RCMT/2001/R112601A.html.
Jaeger, J.C., Cook, N.G.W., 1976. Fundamentals of Rock Mechanics. Halsted, New York, 585 pp.
Kopf, A.J., 2002. Significance of mud volcanism. Reviews of Geophysics 40 (2), 1005, doi:10.1029/2000RG000093.
Liotta, D., 1991. The Arbia-Val Marecchia Line, Northern Apennines. Eclogae Geologicae Helvetiae 84, 413–430.
Lockner, D.A., 1995. Rock failure. In: Ahrens, T.J. (Ed.), Rock Physics and Phase Relations: A Handbook of Physical Constants, vol. 3. American Geophysical Union Reference Shelf, Washington,, pp. 127–147.
Mazzini, A., Svensen, H., Akhmanov, G.G., Aloisi, G., Planke, S., Malthe-Sørenssen, A., Istadi, B., 2007. Triggering and dynamic evolution of the LUSI mud volcano, Indonesia. Earth and Planetary Science Letters 261, 375–388.
Milkov, A.V., 2000. Worldwide distribution of submarine mud volcanoes and associated gas hydrates. Marine Geology 167, 29–42.
Miller, S.A., Collettini, C., Chiaraluce, L., Cocco, M., Barchi, M., Kaus, B.J.P., 2004. Aftershocks driven by a high-pressure CO_2 source at depth. Nature 427, 724–727.
Minissale, A., 2004. Origin, transport and discharge of CO_2 in central Italy. Earth-Science Reviews 66, 89–141.
Neuzil, C.E., 1995. Abnormal pressures as hydrodynamic phenomena. American Journal of Science 295, 742–786.
Petit, J.-P., Wibberley, C.A.J., Ruiz, G., 1999. 'Crack–seal', slip: a new fault valve mechanism? Journal of Structural Geology 21, 1199–1207.
Principi, G., Treves, B., 1984. Il sistema corso-appenninico come prisma d'accrezione. Riflessi sul problema generale del limite Alpi-Appennini. Memorie Società Geologica Italiana 28, 549–576.
Ramsay, J.G., 1980. The crack-seal mechanism of rock deformation. Nature 284, 135–139.
Regione Toscana, 2002–2005. Regional Geological Cartography, scale 1:10,000, available from: http://www.rete.toscana.it/sett/pta/terra/geologia/cartografia.htm.
Ricci Lucchi, F., 1986. The Oligocene to Recent foreland basins of the Northern Apennines. International Association of Sedimentologists Special Publication 8, 105–139.
Sibson, R.H., 1981. Fluid flow accompanying faulting: field evidence and models. In: Simpson, D.W., Richards, P.G. (Eds.), Earthquake Prediction: An International Review, vol. 4. American Geophysical Union Maurice Ewing Series, pp. 593–603.
Sibson, R.H., 1985. A note on fault reactivation. Journal of Structural Geology 27, 751–754.
Sibson, R.H., 1992. Implications of fault valve behaviour for rupture nucleation and recurrence. Tectonophysics 211, 283–293.
Sibson, R.H., 1996. Structural permeability of fluid-driven fault-fracture meshes. Journal of Structural Geology 18, 1031–1042.
Sibson, R.H., 2000. Fluid involvement in normal faulting. In: Cello, G., Tondi, E. (Eds.), The Resolution of Geological Analysis and Models for Earthquake Faulting Studies, 29. Journal of Geodynamics, pp. 469–499.
Sibson, R.H., 2007. An episode of fault-valve behaviour during compressional inversion? – The 2004 M_J6.8 Mid-Niigata Prefecture, Japan, earthquake sequence. Earth and Planetary Science Letters 257, 188–199.
Sorgi, C., Deffontaines, B., Hippolyte, J.C., Cadet, J.P., 1998. An integrated analysis of transverse structures in the northern Apennines, Italy. Geomorphology 25, 193–206.
Tanini, C., 1998. Tettonica Attiva dell'Appennino Centro-Settentrionale compreso fra le province di Arezzo, Perugia e Terni. PhD Thesis, Florence University.
Vaselli, O., Tassi, F., Minissale, A., Capaccioni, B., Magro, G., Evans, W., 1997. Geochemistry of natural gas manifestations from the upper Tiber Valley (Central Italy). Mineralogica et Petrographica Acta 40, 201–212.